Optical Materials 33 (2011) 359–362

Contents lists available at ScienceDirect

Optical Materials

journal homepage: www.elsevier.com/locate/optmat

Enhanced ultraviolet sensitivity of zinc oxide nanoparticle photoconductors by surface passivation

Liqiao Qin, Christopher Shing, Shayla Sawyer *, Partha S. Dutta

Electrical, Computer, and Systems Engineering Department, Rensselaer Polytechnic Institute, Troy, NY 12180, USA

ARTICLE INFO

Article history:
Received 10 August 2010
Received in revised form 17 September 2010
Accepted 20 September 2010
Available online 25 October 2010

Keywords:
Zinc oxide (ZnO) nanoparticles
Polyvinyl-alcohol (PVA)
Ultraviolet (UV) photoconductor
Surface passivation

ABSTRACT

Zinc oxide nanoparticles were created by a top-down wet-chemical etching process and then coated with polyvinyl-alcohol (PVA), exhibiting sizes ranging from 10 to 120 nm with an average size approximately 80 nm. The PVA layer provides surface passivation of zinc oxide nanoparticles. As a result of PVA coating, enhancement in ultraviolet emission and suppression of parasitic green emission is observed. Photoconductors fabricated using the PVA coated zinc oxide nanoparticles exhibited a ratio of ultraviolet photogenerated current to dark current as high as 4.5×10^4, 5 times better than that of the devices fabricated using uncoated ZnO nanoparticles.

1. Introduction

ZnO is a direct wide bandgap semiconductor material with documented bandgap values ranging from 3.2 to 3.4 eV. Various attractive characteristics of ZnO, including large exciton binding energy (60 meV), high radiation hardness, and relatively low growth temperature, have prompted its applications in transparent conducting electrodes (TCOs), varistors, gas sensors, ultraviolet (UV) photodetector, UV light emitting diodes (LEDs), transistors, solar cells, magnetics, biologic, catalysis and devices based on piezoelectricity [1–9]. ZnO nanostructures are especially interesting due to their quantum confinement effects which enable continuous tuning of the emission and detection wavelengths and improved device performance [4–16]. To date, a variety of techniques have been widely used in the synthesis of ZnO nanostructures, including high temperature sputtering [17], molecular beam epitaxy [18], chemical vapour deposition [19], electrophoretic deposition [20], and chemical bath deposition [9,10,16].

Wet chemical synthesis is an inexpensive way to create ZnO nanostructures. Traditional wet-chemistry synthesis is a bottom-up process based on reactions of a variety of precursors using different conditions, such as temperature, time, and concentration of reactants, leading to varying sizes and geometries of the resulting particles. However, there are several significant challenges associated with this method, including difficulty in preparation of a stable dispersion, poor uniformity in the coating process, and poor conductivity of the ZnO thin films (fabricated using the nanoparticles). This is due to imperfect crystalline phases and impurities present in the nanoparticles or adsorbed on the surface. Another prominent issue common to ZnO nano-materials is a strong, parasitic green photoluminescence caused by excess Zn^{2+} ions and oxygen deficiencies [13–15,21], and a lack of stability under ambient conditions [22]. Researchers have begun to investigate the effective use of surface modification [23–25], and annealing treatments [26] to solve parasitic effects. Dutta and co-workers reported a new low temperature top-down wet-chemical etching method to generate controllable and stably dispersed ZnO nanoparticles [16]. This top-down method along with surface coating could resolve these issues while maintaining low cost and ease of fabrication associated with wet chemical processes.

In this paper, the material and device characteristics of polyvinyl-alcohol (PVA) coated ZnO nanoparticles made by a top-down wet-chemical etching method are measured. Polyvinyl-alcohol (PVA) provided significant suppression of the parasitic green emission and enhanced UV emission. Photoconductors based on the ZnO nanoparticles are fabricated and characterized with improved device performance provided by the PVA surface passivation and stable dispersion of the nanoparticles.

2. Experiment

In this study, commercial ZnO particles of average 1–2 μm in sizes were chemically etched to create nanoparticles. The starting ZnO particles were synthesized at a high temperature, giving rise

* Corresponding author. Tel.: +1 518 276 2164; fax: +1 518 276 2990.
E-mail address: ssawyer@ecse.rpi.edu (S. Sawyer).

0925-3467/$ - see front matter © 2010 Elsevier B.V. All rights reserved.
doi:10.1016/j.optmat.2010.09.020

to pure crystalline phases and high purity of the synthesized powders. Using the slow and controllable top-down chemical etching process described here, nanoparticles as small as 10 nm sizes have been demonstrated. To start with, the micron size ZnO particles were suspended in deionized water using a magnetic stirrer. The solid weight percent of the ZnO particles in water was approximately 2.5%. A separate mild acidic solution (pH ~6) was prepared by adding acetic acid in water. The acidic solution was then added drop by drop (at a rate of 2–3 ml every minute) to the ZnO colloidal suspension while the liquid was vigorous stirred. The acetic acid etches ZnO by forming zinc acetate which dissolved in water. After 2 h of etching, the solution was centrifuged and the ZnO particles were extracted. The extracted particles were suspended in deionized water and washed. The solution was then centrifuged and the particles were extracted again. The etching process is repeated several times as described above beginning with suspending the extracted ZnO particles in water and adding acetic acid solution for 2 h. After six etching cycles it was observed that ZnO nanoparticles with size below 100 nm could be obtained. At the end of this etching process, the colloidal suspension was separated into two batches. One batch was surface treated by dissolving PVA (0.5% in weight in water). The PVA capping on the ZnO nanoparticles occurred due to the reaction of excess Zn^{2+} on the surface with the hydroxyl group of the PVA. The particles from both batches [uncoated (ZnO–A) and PVA-coated (ZnO–U)] were centrifuged and dispersed in ethanol to form 30 mg/ml suspension. These solutions were then spin-casted onto quartz plates and annealed in air at 150 °C for 5 min.

Characterization methods used to determine the material quality and optical characteristics of the ZnO nanoparticles are the following. X-ray diffraction (XRD) was performed on a Bruker D8 Discover X-ray diffractometer with a high-star 2-d detector. The 2-theta used in the measurement was from 30° to 100°. The size and morphology of the ZnO nanoparticles were determined using a Carl Zeiss Ultra 1540 dual beam scanning electron microscope (SEM) set to 5 kV. The ZnO nanoparticles were characterized by their excitation and emission spectra using a Spex Fluorolog Tau-3 spectrofluorimeter. UV–Vis absorption spectra were recorded using a Shimadzu UV–Vis 2550 spectrophotometer with a deuterium lamp (190–390 nm) and a halogen lamp (280–1100 nm). Auto switching between the lamps is synchronized to a wavelength and the switching range is selectable between 282 and 393 nm. The scanning wavelength range used in the experiment is 240–800 nm with a switching wavelength of 330 nm.

Photoconductors were made by depositing two irregular 100 nm Al contacts on top of the ZnO nanoparticle film formed as stated above using E-beam via shadow mask. A schematic diagram of the detectors is presented in the inset of Fig. 1(b). Point contact current–voltage (I-V) characteristics of samples were measured using a HP4155B semiconductor parameter analyzer under darkness and under illumination by a 340 nm UV LED with an intensity of 45.58 mW/cm^2. These measurements were performed at room temperature in air.

3. Results and discussion

The XRD pattern of ZnO nanoparticles coated with PVA (ZnO–U) is shown in Fig. 1(a). The peaks coincide with hexagonal zinc oxide (AMCSD#0005163, a = 3.2494 Å, c = 5.2038 Å) of high purity. Fig. 1(b) is a high resolution SEM image of PVA coated ZnO nanoparticles (ZnO–U) spin-casted onto a quartz plate. The sizes of the nanoparticles are in the range of 10–150 nm with an average value of approximately 80 nm. Uncoated ZnO nanoparticles (ZnO–A) in ethanol spin-casted on quartz plates exhibit a similar size.

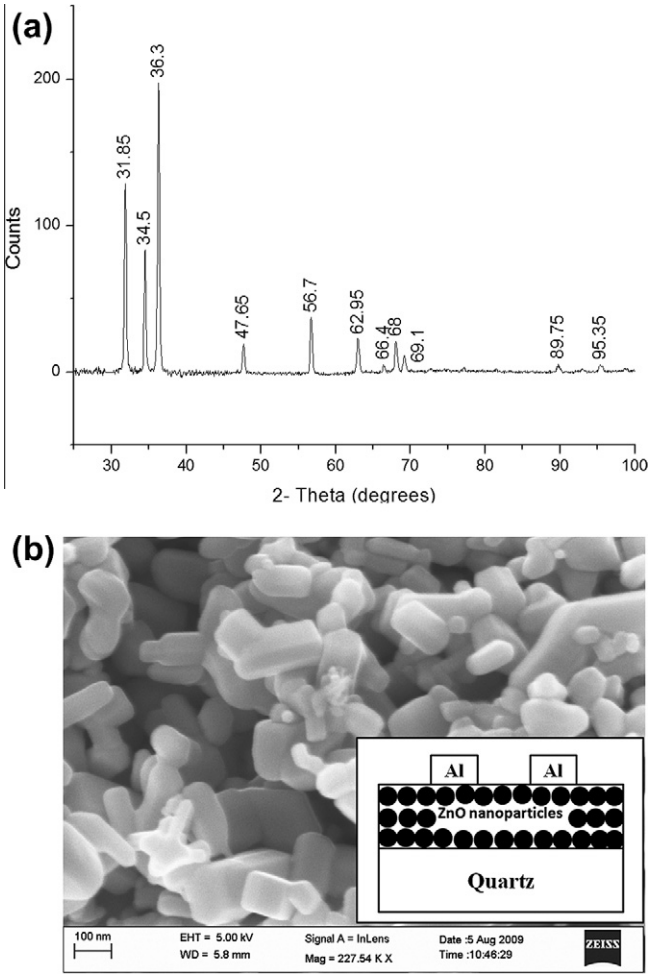

Fig. 1. (a) XRD patterns (b) High resolution SEM results, of PVA coated ZnO nanoparticles (ZnO–U) created by top-down wet-chemical synthesis with an average size of 80 nm (the inset is the schematic diagram of the photoconductors).

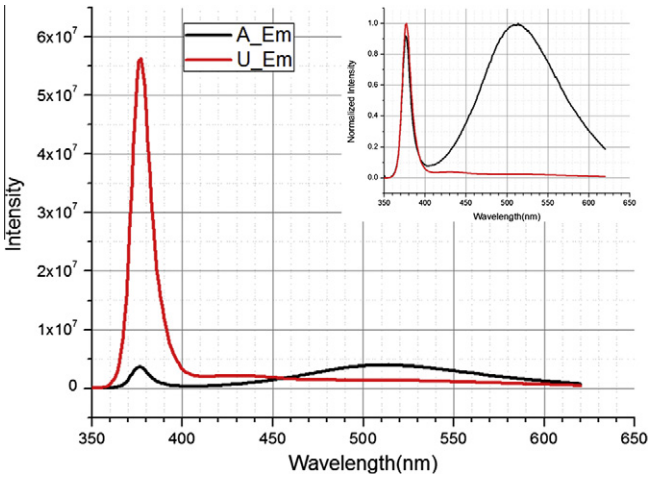

Fig. 2. Emission spectra of ZnO excited at 340 nm indicating enhanced UV and suppressed green emission in PVA coated ZnO nanoparticles (ZnO–U) in contrast to uncoated ZnO nanoparticles (ZnO–A) (the inset is the normalized spectra).

The emission spectra of the uncoated ZnO nanoparticles (ZnO–A), shown in Fig. 2, demonstrate two transitions exist: a near-band-edge UV transition and a broad green emission caused

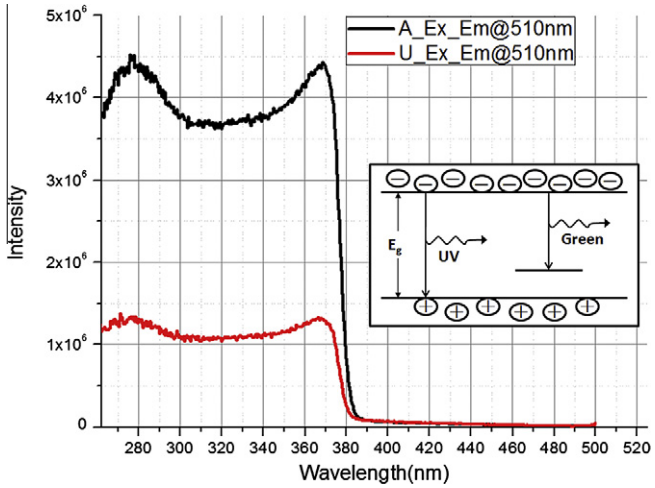

Fig. 3. Excitation spectra of ZnO (λ_{em} = 510 nm) (the inset schematically shows the near-band-edge and the green emission of ZnO, respectively).

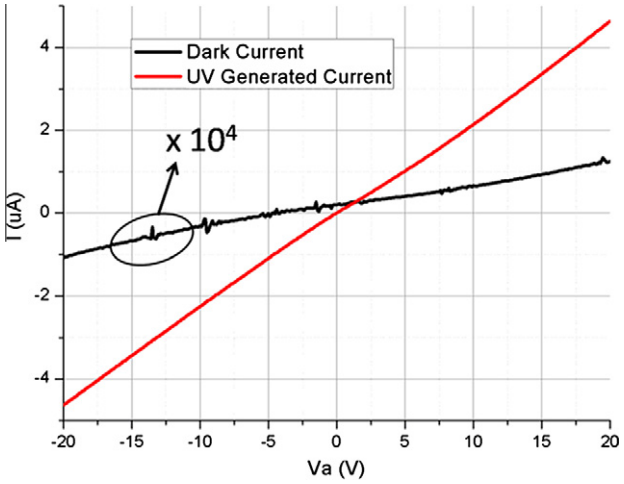

Fig. 5. I–V plot of photodetector based on PVA coated ZnO nanoparticles (ZnO–U) shows a linear I–V response and the UV generated current to dark current ratio over four orders.

by deep level defects. This corresponds with the transitions shown in the Fig. 3 inset of the ZnO band diagram. When excited at 340 nm, the emission spectra clearly indicate an enhanced UV and a diminished parasitic green emission occurs in PVA coated ZnO nanoparticles (ZnO–U) compared with uncoated ZnO nanoparticles (ZnO–A). The ratio of UV emission peak (377 nm) to the green emission peak (520 nm) increased from 0.93 in uncoated ZnO nanoparticles (ZnO–A) to 40.85 in PVA coated ZnO nanoparticles (ZnO–U).

The excitation spectra of the ZnO nanoparticles are shown in Fig. 3. When the emission wavelength was set at 510 nm (around the peak of the parasitic green emission of ZnO) the excitation spectra indicated most of the parasitic green emission comes from UV excitation. The UV-excited electrons in the conduction band cannot recombine with the holes in the valence band since they are trapped by the holes in the deep level defects of ZnO. However, the green emission from uncoated ZnO nanoparticles (ZnO–A) is about 4 times of that from PVA coated ZnO nanoparticles (ZnO–U). This indicates the PVA coating helps passivate the surface of ZnO nanoparticles by decreasing the number of holes in the deep level and thus reducing the parasitic green photoluminescence of

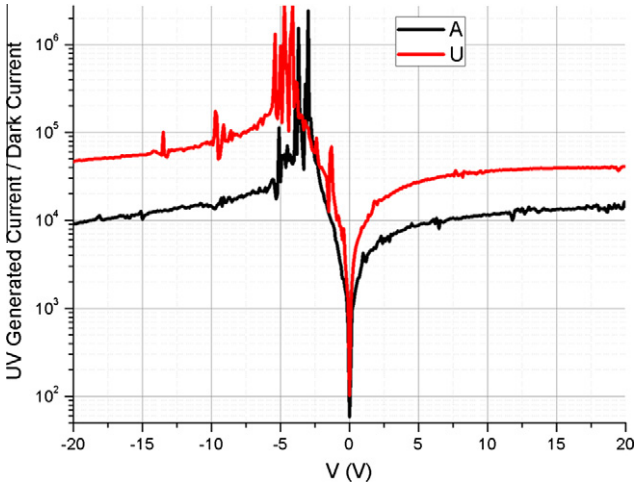

Fig. 6. The ratio of UV generated current to dark current of photodetector based on uncoated ZnO nanoparticles (ZnO–A) and PVA coated ZnO nanoparticles (ZnO–U) respectively.

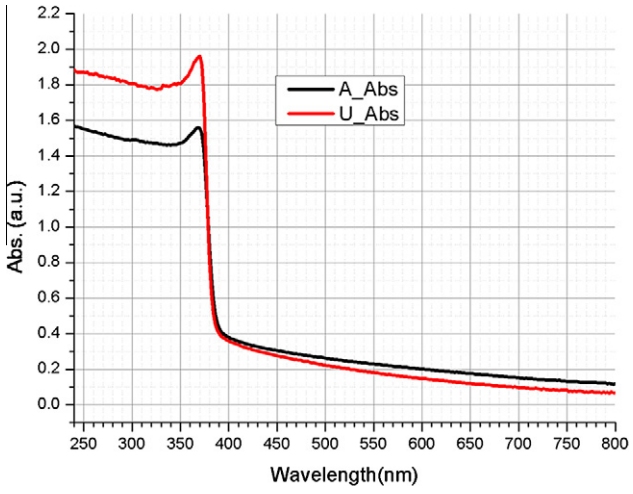

Fig. 4. Absorption spectra of ZnO demonstrate higher UV and lower visible absorption in PVA coated ZnO nanoparticles (ZnO–U) comparing with uncoated ZnO nanoparticles (ZnO–A).

ZnO following UV-excitation. Excess Zn^{2+} is normally considered the major contributor to green emission since the dangling bonds form the donor states in ZnO that easily trap the UV-excited electrons [13–15,21,27,28]. Therefore the suppressed green emission observed in PVA coated ZnO nanoparticles (ZnO-U) indicates PVA is an effective surface passivation material to ZnO and has a strong interaction with excess Zn^{2+}.

As demonstrated in Fig. 4, there is no significant difference in the absorption spectra of uncoated ZnO nanoparticles (ZnO–A) and PVA coated ZnO nanoparticles (ZnO–U), although PVA coated ZnO nanoparticles (ZnO–U) exhibits an increase in UV absorption and a slight decrease in visible wavelength absorption. The absorption spectra shows the cut-off wavelengths for both samples to be around 375 nm, a 5 nm blue shift compared with the bulk material (380 nm). This indicates the presence of nano-scale particles (as shown in the high resolution SEM results of Fig. 1(b)) and their corresponding quantum confinement effect in these samples.

Fig. 5 is a typical I–V curve of photoconductors based on ZnO nanoparticles under dark and illuminations of 340 nm UV LED with an intensity of 45.58 mW/cm^2. The linear I–V responses show that a photoconductor based on ZnO nanoparticles and Al contacts has

been achieved. The ratios of UV photo-generated current to dark current (on/off ratio) are shown in Fig. 6. In uncoated ZnO nanoparticles (ZnO–A), the ratio is about 9×10^3 when the bias is -20 V. Meanwhile, for PVA coated ZnO nanoparticles (ZnO–U) the ratio is as high as 4.5×10^4, 5 times that of uncoated ZnO nanoparticles (ZnO–A). Since most of the UV-generated carriers in the ZnO are trapped by defects during transportation to the terminals and uncoated ZnO nanoparticles (ZnO–A) has a higher surface defect concentration than PVA coated ZnO nanoparticles (ZnO–U), this increased ratio is expected. However, the dark currents of both detectors are about 100pA at -20 V bias. This indicates PVA does not change the conductivity of ZnO nanoparticles, but acts as an effective surface passivation material to improve the photosensitivity of ZnO nanoparticles. The charge transport mechanism across the ZnO/PVA/Al is still under investigation. However, it is speculated that it could be due to tunnelling.

4. Conclusion

In conclusion, enhanced UV emission and suppression of parasitic green photoluminescence has been observed in PVA coated ZnO nanoparticles prepared using a top-down wet-chemical etching process. Photoconductor based on PVA coated ZnO exhibited increase in photocurrent sensitivity. These results indicate that PVA coating of ZnO nanoparticles could be applied in creating low cost, sensitive and visible blind UV photodetectors.

Acknowledgements

The authors gratefully acknowledge support from National Security Technologies through NSF Industry/University Cooperative Research Center Connection One. The authors also acknowledge the National Science Foundation Smart Lighting Engineering Research Center (EEC-0812056).

References

[1] J. Sheu, M. Lee, C. Tun, S. Lin, Appl. Phys. Lett. 88 (2006) 043506.
[2] P. Durán, F. Capel, J. Tartaj, C. Moure, Adv. Mater. 14 (2002) 137.
[3] D. Lin, H. Wu, W. Zhang, He. Li, W. Pan, Appl. Phys. Lett. 94 (2009) 172103.
[4] E. Neshataeva, T. Kümmell, G. Bacher, A. Ebbers, Appl. Phys. Lett. 94 (2009) 091115.
[5] S. Lee, Y. Jeong, S. Jeong, J. Lee, M. Jeon, J. Moon, Superlatt. Microstruc. 44 (2008) 761.
[6] M. Wang, Y. Lian, X. Wang, Curr. Appl. Phys. 9 (2009) 189.
[7] X. Zhua, I. Yurib, X. Gana, I. Suzukib, G. Lia, Biosens. Bioelectron. 22 (2007) 1600.
[8] Y. Qin, X. Wang, Z. Wang, Nature 451 (2008) 809.
[9] Y. Jin, J. Wang, B. Sun, J. Blakesley, N. Greenham, Nano Lett. 8 (2008) 1649.
[10] Y. Lin, C. Chen, W. Yen, W. Su, C. Ku, J. Wu, Appl. Phys. Lett. 92 (2008) 233301.
[11] G. Cheng, Z. Li, S. Wang, G. Gong, K. Cheng, X. Jiang, S. Zhou, Z. Du, T. Cui, G. Zou, Appl. Phys. Lett. 93 (2008) 123103.
[12] J. Jun, H. Seong, K. Cho, B. Moon, S. Kim, Ceram. Int. 35 (2009) 2797.
[13] S. Monticone, R. Tufeu, A. Kanaev, J. Phys. Chem. B 102 (1998) 2854.
[14] Y. Wu, A. Tok, F. Boey, X. Zeng, X. Zhang, Appl. Surf. Sci. 253 (2007) 5473.
[15] L. Wu, Y. Wu, X. Pan, F. Kong, Opt. Mater. 28 (2006) 418.
[16] S. Sharma, A. Tran, O. Nalamasu, P. Dutta, J. Electron. Mater. 35 (2006) 1237.
[17] Z. Bi, J. Zhang, X. Bian, D. Wang, X. Zhang, W. Zhang, Z. Hou, J. Electron. Mater. 37 (2008) 760.
[18] W. Heo, V. Varadarajan, M. Kaufman, K. Kim, D. Norton, F. Ren, P. Fleming, Appl. Phys. Lett. 81 (2002) 3046.
[19] A. Umar, S. Lee, Y. Lee, K. Nahm, Y. Hahn, J. Cryst. Growth 277 (2005) 479.
[20] Y. Wang, I. Leu, M. Hon, Electrochem. Solid-State Lett. 5 (2002) 53.
[21] K. Borgohain, S. Mahamuni, Semicond. Sci. Technol. 13 (1998) 1154.
[22] D. Talapin, A. Rogach, E. Shevchenko, A. Kornowski, M. Hasse, M. Hasse, H. Weller, J. Am. Chem. Soc. 124 (2002) 5782.
[23] H. Xiong, Z. Wang, Y. Xia, Adv. Mater. 18 (2006) 748.
[24] L. Guo, S. Yang, C. Yang, P. Yu, J. Wang, W. Ge, G. Wong, Appl. Phys. Lett. 76 (2000) 2901.
[25] S. Mridha, M. Nandi, A. Bhaumik, D. Basak, Nanotechnology 19 (2008) 275705.
[26] S. Venkataprasad Bhat, S.R.C. Vivekchand, A. Govindaraj, C.N.R. Rao, Solid State Commun. 149 (2009) 510.
[27] V.A. Fonoberov, A.A. Balandin, Appl. Phys. Lett. 85 (2004) 5971 (2004).
[28] V.A. Fonoberov, K.A. Alim, A.A. Balandin, Phys. Rev. B 73 (2006) 165317.